

Supplementary Information

Shape-Controlled Synthesis of TiO₂ Hollow Structures and Their Application in Lithium Batteries

Yong Wang,* Xiaowen Su, and Shan Lu

Department of Chemistry, Capital Normal University, Beijing 100048, P. R. China,
E-mail: yongwang@home.ipe.ac.cn.

S1. XRD patterns of monodisperse Fe_2O_3 particles with different shapes

Fig. S1 displays the X-ray diffraction (XRD) patterns of the as-obtained samples. In Fig. S1, all the as-obtained samples are identified as the single phase $\alpha\text{-Fe}_2\text{O}_3$ with well-crystallized rhombohedral structure ($a=0.5038$ nm, $c=1.3772$ nm, JCPDS file No. 24-0072). No peaks from other phases are found, suggesting high purity of the final products.

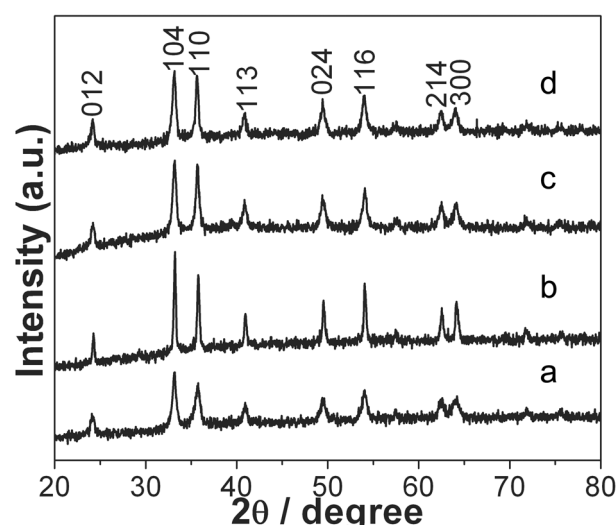


Fig. S1 XRD patterns of monodisperse Fe_2O_3 particles with different shapes: (a) peanuts; (b) capsules; (c) ellipsoids; and (d) pseudocubes.

S2. XRD patterns of monodisperse $\alpha\text{-Fe}_2\text{O}_3/\text{TiO}_2$ core/shell particles with different shapes

The crystallographic structures of the as-formed $\alpha\text{-Fe}_2\text{O}_3/\text{TiO}_2$ core/shell particles with different shapes in the second step are determined by X-ray diffraction (XRD) analysis. In Fig. S2, all of the peaks observed can be unequivocally assigned to $\alpha\text{-Fe}_2\text{O}_3$ with rhombohedral structure ($a=0.5038$ nm, $c=1.3772$ nm, JCPDS file No. 24-0072, signal #) and anatase TiO_2 with tetragonal structure ($a=0.37892$ nm, $c=0.9537$ nm, JCPDS file No. 71-1167, signal +).

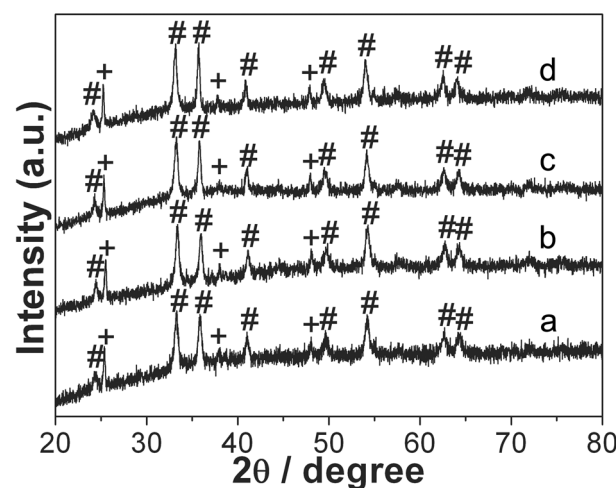


Fig. S2 XRD patterns of monodisperse $\alpha\text{-Fe}_2\text{O}_3/\text{TiO}_2$ core/shell with different shapes: (a) peanuts; (b) capsules; (c) ellipsoids; and (d) pseudocubes. Fe_2O_3 (#) and TiO_2 (+).

S3. FESEM images and EDX spectra of monodisperse α -Fe₂O₃/TiO₂ core/shell particles with different shapes

The morphology and structure of the samples were further investigated by field emission scanning electron microscopy (FESEM, Hitachi, S-4800) with energy-dispersive X-ray (EDX) spectroscopy. The element composition is further confirmed by energy dispersive X-ray (EDX) spectroscopy analysis. EDX point spectra taken from the center point of a core/shell particle and line scans show strong Fe, Ti and O signals (Fig. S3). Au peaks have been observed in EDX analysis because of the gold coating deposited on the samples before FESEM/EDX analysis. Al peaks are attributed to the aluminum foil used as the holder. As shown in Fig. S3j-l, a broken α -Fe₂O₃/TiO₂ core/shell particle with pseudocube-shape can be observed. It is noted that Fe signal strengthens and Ti signal weakens beside the broken part (Fig. S3l), which further confirms the formation of α -Fe₂O₃/TiO₂ core/shell particles.

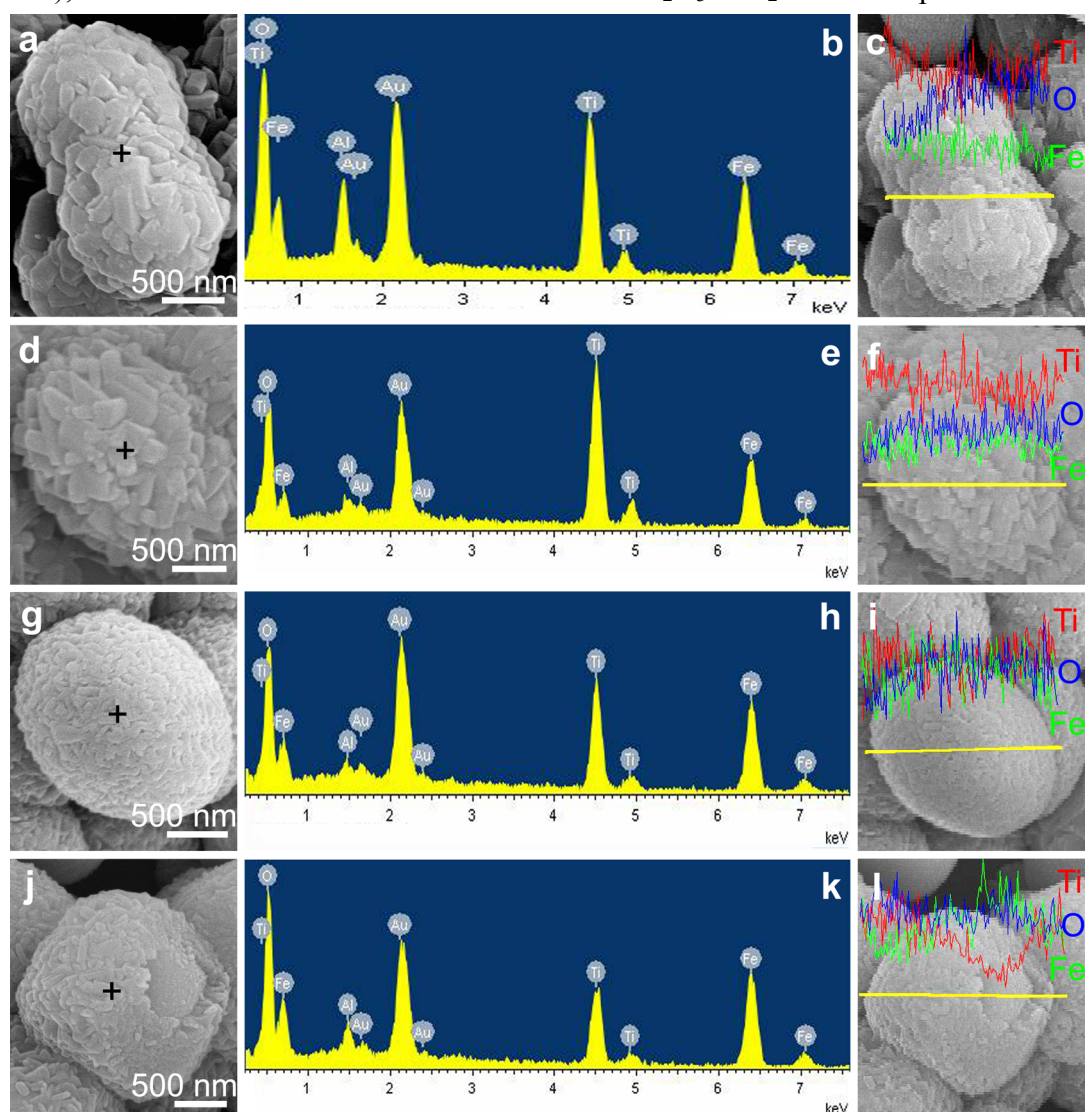


Fig. S3 FESEM images, EDX point spectra and line scans of monodisperse α -Fe₂O₃/TiO₂ core/shell with different shapes: (a-c) peanuts; (d-f) capsules; (g-i) ellipsoids; and (j-l) pseudocubes. Al peaks are attributed to the aluminum foil used as the holder. The Au peaks are from the conducting layer of Au used for FESEM characterization. (b), (e), (h) and (k) are EDX point spectra taken from the center point of a core/shell particle marked with a cross in the FESEM images of (a), (d), (g) and (j), respectively.

S4. EDX spectra of TiO₂ hollow particles with different shapes under TEM

The element composition is further confirmed with energy dispersive X-ray (EDX) spectroscopy analysis under TEM. EDX point spectra, taken from the center point of a hollow particle, show strong Ti and O signals (Fig. S4), and no Fe signal is found, which demonstrates the complete removal of Fe₂O₃ and the formation of TiO₂ hollow particles with different shapes. The Cu and C peaks are attributed to the carbon-coated Cu grid used in TEM.

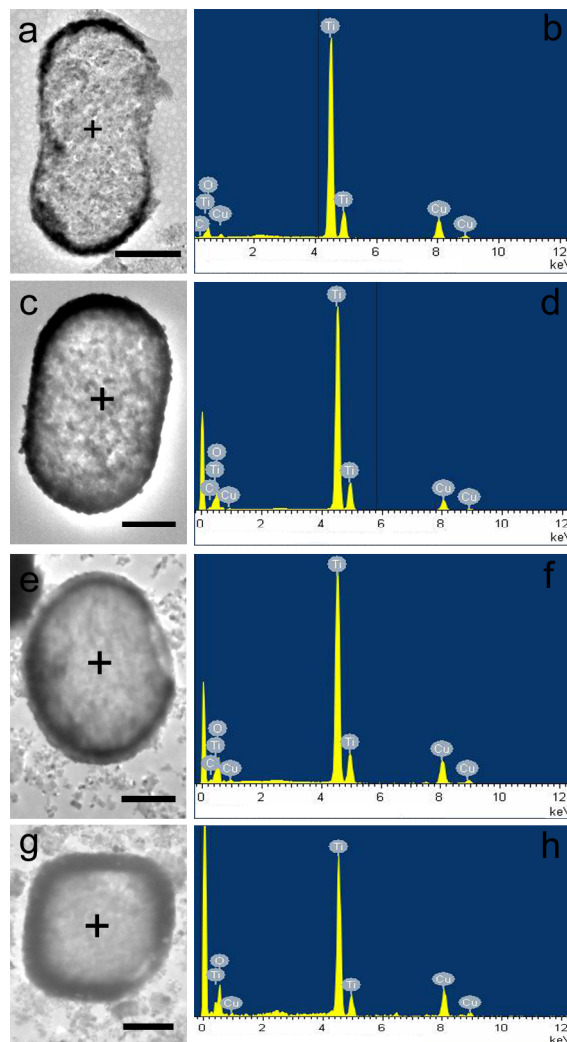


Fig. S4 TEM images and EDX point spectra of TiO₂ hollow particles with different shapes: (a-b) peanuts; (c-d) capsules; (e-f) ellipsoids; and (g-h) pseudocubes. The Cu and C peaks are attributed to the carbon-coated Cu grid used in TEM. (b), (d), (f) and (h) are EDX point spectra taken from the center point of a TiO₂ hollow particle marked with a cross in the TEM images of (a), (c), (e) and (g), respectively. All of the scale bars are 500 nm.

S5. Coulombic efficiencies of TiO₂ hollow particles with different shapes and solid microspheres

As shown in Fig. S5, the coulombic efficiencies of these TiO₂ hollow particles and solid microspheres are in the range of 70 to 80% in the first cycle, which increase to 93-97% in the second cycle and maintain in the range of 98 to 100% for the rest cycles.

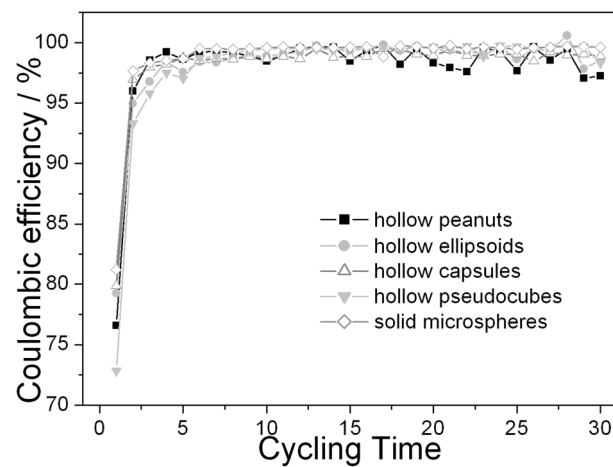


Fig. S5 Coulombic efficiency of TiO₂ hollow particles with different shapes and solid microspheres.